"Smart" baroreception along the aortic arch, with reference to essential hypertension

G. C. Kember,[1] M. Zamir,[2] and J. A. Armour[3]
[1]*Department of Engineering Mathematics, Dalhousie University, P.O. Box 1000, Halifax, Nova Scotia, Canada B3J 2X4*
[2]*Department of Applied Mathematics, University of Western Ontario, London, Ontario, Canada N6A 5B7*
[3]*Department of Pharmacology, University of Montreal, Montreal, Quebec, Canada H3C 3J7*
(Received 12 September 2003; revised manuscript received 18 May 2004; published 24 November 2004)

Beat-to-beat regulation of heart rate is dependent upon sensing of local stretching or local "disortion" by aortic baroreceptors. Distortions of the aortic wall are due mainly to left ventricular output and to reflected waves arising from the arterial tree. Distortions are generally believed to be useful in cardiac control since stretch receptors or aortic baroreceptors embedded in the adventitia of the aortic wall, transduce the distortions to cardiovascular neural reflex pathways responsible for beat-to-beat regulation of heart rate. Aortic neuroanatomy studies have also found a continuous strip of mechanosensory neurites spread along the aortic inner arch. Although their purpose is now unknown, such a combined sensing capacity would allow measurement of the space and time dependence of inner arch wall distortions due, among other things, to traveling waves associated with pulsatile flow in an elastic tube. We call this sensing capability–"smart baroreception." In this paper we use an arterial tree model to show that the cumulative effects of wave reflections, from many sites *far downstream*, have a surprisingly pronounced effect on the *pressure distribution* in the root segment of the tree. By this mechanism global hemodynamics can be focused by wave reflections back to the aortic arch, where they can rapidly impact cardiac control via smart baroreception. Such sensing is likely important to maintain efficient heart function. However, alterations in the arterial tree due to aging and other natural processes can lead in such a system to altered cardiac control and essential hypertension.

DOI: 10.1103/PhysRevE.70.051914 PACS number(s): 87.19.Hh

I. INTRODUCTION

Spinal cord and brain stem reflexes continuously modulate cardiodynamics. Fast-responding reflexes involving medullary neurons respond to inputs from carotid artery baroreceptors and account for beat-to-beat control of heart rate and its variability [1–5]. These medullary neurons are known to undergo threshold resetting in *response* to change in sensory input during the evolution of essential hypertension [2,4,6]. It has also been proposed that blunting of baroreflex control may also be a *cause* of cardiac pathology [7].

To date, it has been assumed that aortic baroreception functions in the same way as baroreception in the carotid artery where "point" or "local" measurement of wall stretch is transduced by physically localized sensory neurites. Yet, with respect to aortic baroreception, one *also* observes a field of sensory neurites arranged as a *strip* along the inner aortic arch. Such an arrangement is clearly capable of producing snapshots of the evolving spatial *pressure distribution* along the inner aortic arch to produce what we term "smart baroreception." "Smart" because global information derived from wave reflections from downstream in the arterial tree is focused back up the arterial tree to the level of the aorta. However, the prevailing notion is that aortic flows are largely dominated by local conditions associated with left ventricle output with a small contribution from wave reflections from the first aortic bifurcation. Under these assumptions, localized wall distortion, as measured by arterial baroreceptors is used to infer bulk flow in an essentially rigid tube. We propose that the accumulated influence of travelling wave reflections emanating from *far downstream* can significantly alter blood flow within the aorta. In this paper we postulate, and later demonstrate, that the pressure distribution along the aortic arch is determined not only by local conditions but, because of wave reflections, by global conditions far downstream. In this framework, global arterial conditions play a role in cardiac control and this provides a physiological motivation for smart baroreception.

II. ARRAY ANATOMY

The relevance of smart baroreception to cardiovascular control stems from the strategic location of mechanosensory neurites and their transduction capabilities. The mechanosensory neurites associated with aortic mechano-transducing afferent neurons display a unique anatomy with sensory neurites distributed primarily along the inner curvature of the aortic arch. These neurites are located in the adventitia of the aorta (i.e., embedded in the fibrous tissue in its outer wall) primarily, but not exclusively, along its *inner* curvature. In this location a "strip" of pressure sensors is distributed in an uninterrupted fashion as the outer curvature of the aorta is "interrupted," so to speak, by the origins of the major arteries that supply blood to the head, neck and upper limbs.

The afferent, innervated aorta is estimated be about 150 mm in length [11]. Because this array of mechanosensory neurites covers approximately $2/5$ of the aorta in this region (the outer curvature being relatively unrepresented), it is estimated that the array transduces mechanical events arising in approximately 500 square mm of the thoracic aorta. The area of the aortic mechanosensory field associated with each mechanosensory neuron has been estimated, by direct probing, to be of the order of one square millimeter. Each of these sensory fields is approximately elliptical in form, with

their major axes lying in the axial rather than the circumferential aortic direction. Each sensory field is associated with a single axon leading to one somata (neuron). It has been also found that the majority of their somata are located adjacent to the aorta, in the middle cervical and stellate ganglia [8,9] versus dorsal root or nodose ganglia [10]. Thus, the axons connecting these mechanosensory neurites with their associated somata are short (about 1–5 cm). Furthermore, they are fast conducting axons, falling into the A-delta class of fibers. Short A-delta axonal lengths between sensory neurites and somata makes possible the rapid transduction of regional aortic mechanics and the initiation of short-latency aortic-cardiac reflexes.

III. ARRAY FUNCTION

Sensing of aortic wall deformation is nearly homogeneous among these afferent neurons in that each mechanosensory neuron transduces wall deformation in a very similar fashion [11]. This is consistent with the relative homogeneity of the anatomy of the thoracic aorta [12]. The functional significance of this anatomy may be explained in terms of: (i) the transduction capability of individual aortic mechanosensory neurons and (ii) the nature of multiple, strip activities generated by this relatively uniform population of afferent neurons.

There is a clear relationship between the activity generated by individual aortic mechano-transducing sensory neurons and aortic wall deformation [13]. Because the elastic properties of that aortic segment are relatively uniform [12], its mechanosensory neurites are distorted to the same degree for a given pressure [13]. Thus, each sensory neurite field is capable of transducing forward pressure waves (peak aortic pressure and the subsequent dicrotic notch) as well as later occurring reflected pressure waves with precision [11]. The physical separation of the sensory fields associated with each mechanosensory afferent neuron, which is of the order of millimeters, allows sufficiently accurate transduction of pressure amplitude *distribution*.

The adjacency of mechanosensory fields to their somata and the fact that these anatomically distinct features of an afferent neuron are connected by a relatively short, rapidly conducting (A-delta) axon ensures that pressure wave transduction occurs at acceptable levels to second order neurons in adjacent intra-thoracic ganglia. The second order computation based on this information occurs among populations of middle cervical and stellate ganglion local circuit neurons. From there it is fed to intrathoracic sympathetic efferent neurons involved in regulating regional cardiac dynamics during each cardiac cycle.

IV. MODEL

To demonstrate how events in the periphery of the aorta and major arteries affect the pressure distribution along the aortic arch and, as a consequence, can be transduced by a strip of mechanosensory neurons, we consider a vascular tree model with vessel dimensions of the same order as those identified in the human aorta and its major branches.

It is important to emphasize at the outset that the purpose of this model is not to replicate the physiological system, but rather to replicate the *mechanisms* by which peripheral dynamics produce changes in the pressure distribution in the intrathoracic aorta. An accurate reproduction of wave propagation along the aorta and its branches would require, among other things, more accurate representation of the fluid and of vessel geometry and elasticity. Indeed, the number of unknowns is such that it is rarely possible to accurately reproduce the flow. However, this is unnecessary for demonstrating the main point of this paper, namely that hemodynamic events in the periphery can produce changes in the pressure distribution far upstream, along a segment of the aortic arch. The assumption of an ideal fluid used in this model equation (3) is a fairly common one when dealing with wave propagation along a tree structure. Also, it has been shown conclusively that including viscosity of the fluid does not change the main pattern of propagation and would not change the main conclusions of this work [14,15]. The analysis of wave propagation along a highly branched tree structure is, by necessity, a one-dimensional problem.

The key mechanism at play here is wave reflections. These arise because of the pulsatile nature of the flow and because of the many obstacles (in the form of vascular junctions) which the propagating wave meets on its way from the root segment of the tree to the periphery. As the pressure wave meets these obstacles, parts of the wave are reflected back (upstream) towards the root segment of the tree [16]. This occurs at each vascular junction. Because of the large number of such junctions, their cumulative effect can be determined only by calculating the effect of each junction and then summing up to determine the total effect. Here again it is not our intention (indeed it is hardly possible) to replicate the number of junctions in the physiological system. It is in fact not necessary to do that in order to demonstrate the proposed transduction mechanisms.

One characteristic of the model which must be physiologically sound is the approximate dimensions of the vessels utilized in the model. This is because wave reflections depend critically on the ratio of wave length to vessel length, while the wave speed, and hence the wave length, depends on the diameters and lengths of the vessels as well as their elasticity. For that reason, we use a highly simplified vascular tree model that consists of 9 levels [15] of repeated bifurcations in which the dimensions of the root segment are of the same order of magnitude as those of the aorta. The ratio of diameters of the two branches at each bifurcation is $1/2$, as shown schematically in Fig. 1. The progression from one level of the tree to the next follows simple optimality rules which have been found to prevail within the vascular tree [17]. A similar model was used successfully to demonstrate the well known "peaking effect," which results from wave reflections in the human aorta and its branches [15].

V. ANALYSIS

The analysis begins with the input of a single harmonic pressure wave into the root segment of the tree and from there the wave propagates towards the periphery. The wave

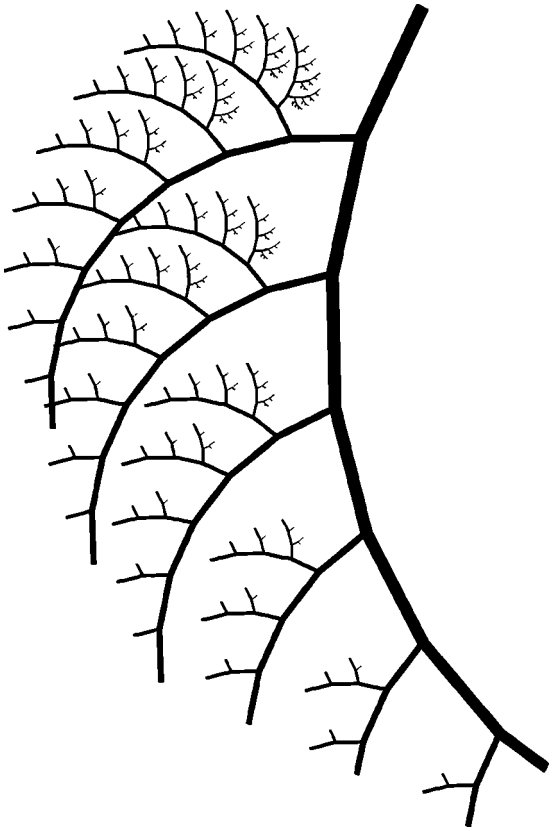

FIG. 1. A vascular tree model consisting of 9 levels of repeated bifurcations in which the ratio of diameters of the two branches at each bifurcation is 1/2, and the progression from one level of the tree to the next follows simple optimality rules which have been found to prevail within the vascular tree (see text).

speed at each vessel segment is determined by the properties of that segment, and the reflection coefficient at each vascular junction is determined by the properties of that junction. Thus the properties of the wave are calculated as it progresses, the most important property being the wave amplitude because the values of the amplitude at different points along each vessel segment and along the tree as a whole determine what we shall refer to as the "pressure distribution." Such a pressure distribution initially determined by the forward moving wave is modified considerably by the multiplicity of reflected waves moving back from vascular junctions. It is this effect that ultimately determines upstream events in the root segment of the tree and is sensed by the strip of mechanosensory neurites located there.

The pressure distribution in each segment of the tree model is determined by the input pressure to that segment and the reflection coefficient at the downstream end of the segment. Thus, the analysis begins with the input pressure $p_0(t)$ to the root segment, which is the input to the entire model. For the purpose of wave propagation analysis, the form of $p_0(t)$ is appropriately taken as a single harmonic, and it is more convenient to put this in the form of a complex exponential:

$$p_0 = p_{00}e^{i\omega t}, \tag{1}$$

where p_{00} is the amplitude of the oscillatory input pressure, ω is the frequency of oscillation, t is time, and $i=\sqrt{-1}$.

Following a standard solution of the wave equation for the pressure, the pressure distribution in each vessel segment is then given by [15,16]

$$p(x,t) = p_0\{e^{i\omega(t-x/c)} + Re^{i\omega[t+(x-2L)/c]}\}, \tag{2}$$

where x is axial distance along that vessel segment, measured from the entrance and being equal to L at exit, R is the reflection coefficient at the downstream end of the segment, and c is the wave speed within the segment. In a tree structure this formula applies to every vessel segment within the tree but the input pressure p_0 and the reflection coefficient R must be calculated individually for each vessel segment. The reflection coefficients are calculated by starting at the periphery and using prescribed mechanical properties of vessel segments to determine characteristic and effective impedances on which the reflection coefficients depend. The input pressures are then calculated by starting at the root segment of the tree and using Eq. (2) to determine the pressure distribution in that segment and hence the input pressure for the next vessel segment, and then the process is repeated for each vessel segment, moving sequentially towards the periphery [16].

Assuming the wall thickness-to-diameter ratio of the vessels is small, the speed is determined by the Moen-Korteweg formula [15,16]

$$c = \sqrt{\frac{Eh}{\rho d}}, \tag{3}$$

where ρ is fluid density, taken as 1.0 g/cm^3, E is the modulus of elasticity, h is the wall thickness and d the diameter of the vessel segment. The use of the Moen-Korteweg formula for the wave speed is a fairly reasonable practice in one dimensional wave propagation. It has been shown that the formula can be extended to include effects of viscosity of the fluid and viscoelasticity of the vessel wall, but the results do not invalidate the formula [14,15]. Indeed, they actually support its wide use except, as was stated above, when one is interested in accurately reproducing the actual pressure distribution along the arch. Such reproduction is not the focus here since our objective is only to show that events far downstream can significantly change the pressure distribution.

In this analysis, the oscillatory part of the pressure and flow is being considered in isolation from the steady part of the flow. The reason for this is that only the oscillatory part of the flow is affected by wave reflections and any pressure changes produced by these will simply add to the pressure distribution associated with the steady part of the flow. Another way of putting this is that the steady part of the flow is affected only by the resistance of the vascular tree, while the oscillatory part is affected by its impedance.

In order to demonstrate the effects of peripheral events on the pressure distribution along the root segment of the tree we calculate the pressure distribution in that segment first using the properties initially assigned to vessel segments,

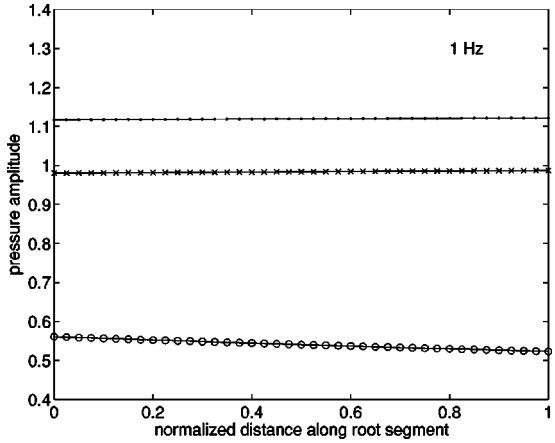

FIG. 2. See Fig. 4 caption.

then with modified properties. In the latter step we consider two scenarios: one in which the peripheral vessels in the last four generations are constricted (diameters reduced by 50%); and one in which the same vessels are stiffened (modulus of elasticity increased from 10^7 to 10^8 g cm/s^2).

The calculations are repeated at three different frequencies, representing low (1 Hz), medium (5 Hz) and high (10 Hz) frequencies, while the results are shown in Figs. 2–4. The reason for using different frequencies is that the cardiac pressure wave consists of a series of harmonic components with a wide range of frequencies. The range of 1–10 Hz is generally believed to represent the major sample of frequencies contained in the composite wave. The results, as illustrated in Figs. 2–4, indicate that the distribution of pressure amplitude along the root segment of the vascular tree model changes considerably when the peripheral vessel segments are constricted or stiffened. We note that the change occurs at all three frequencies. It thus follows that a composite wave consisting of harmonic components with this range of frequencies will change its shape along the root segment of the tree. Our hypothesis is that this change will be sensed with smart baroreception associated with a strip of sensory neurites spread along that segment.

The underlying concept, that changes in vascular properties can be 'sensed' upstream, is not a new one. Indeed,

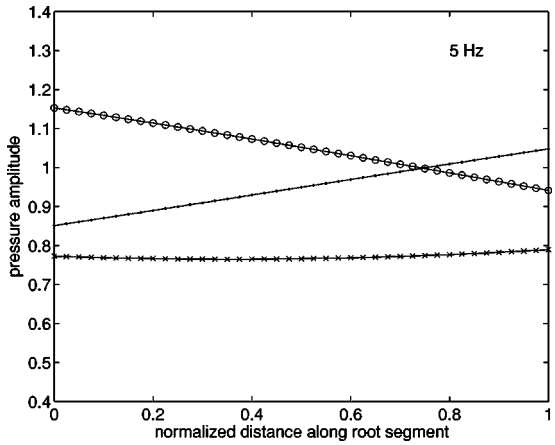

FIG. 3. See Fig. 4 caption.

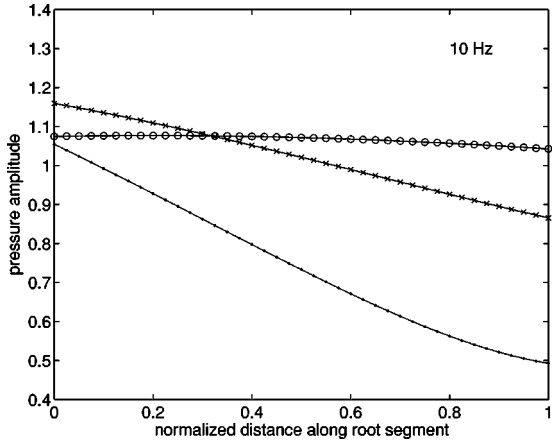

FIG. 4. The pressure amplitude distribution is depicted in Figs. 2–4 for the root segment of the tree model in Fig. 1. The curves with open circles show the distribution under originally prescribed conditions, those with dots show the distribution when peripheral vessels are constricted, and those with crosses show the distribution when the peripheral vessels are stiffened. The distributions shown in the three figures correspond to low (1 Hz), moderate (5 Hz), and high (10 Hz) frequency, as indicated in each figure.

Nicols and O'Rourke [18] state that "Palpation of the arterial pulse is a routine part of the clinical examination, rooted in antiquity," and "Changes in contour of the arterial pulse are usually due to changes in vascular properties, with relatively less or more, or relatively early or later, wave reflections." The purpose of our analysis is to demonstrate how this can happen and, in doing so, give credence to this concept and the fact that such events are available for sensory transduction.

VI. CONCLUSIONS

We have used an arterial tree model to demonstrate that global events, far downstream of the aorta, can almost instantaneously cause significant alterations in the blood flow regime at the aortic level. The accumulated effect of backward traveling waves, generated by reflections from branching points in the arterial tree, is shown to have a surprisingly large impact on the aortic pressure distribution. In this way, dynamical information can be relayed from the arterial tree periphery and focused at the level of the aortic arch where it is sensed as aortic wall distortions by the strip of mechanosensory neurites found on the aortic inner arch. The speed by which the wave reflection effects from the outer periphery reach the inner aortic arch is fast enough to affect adrenergic cardiac motor neurons regulating short-term heart rate variation [19]. We have termed this sensing "smart" baroreception in order to distinguish it from carotid "point" baroreception.

Although much work needs to be done to quantify the role of smart baroreception in cardiac control, it is shown here that smart baroreception strongly depends upon arterial tree properties such as elasticity and geometry. Changes in these properties could prompt smart baroreception to inappropriately reset in much the same way that carotid bulb baroceptors are known to reset in response to underlying arterial

stiffening ([5,6]). For example, stiffening of the thoracic aortic wall would cause a relative reduction in local wall distortion and a reduced capacity to transduce aortic pressure events. This altered state might be analogously overcome by increasing reflex drive to cardiac sympathetic efferent neurons with the aim of reestablishing previously "normal" aortic wall deformation. The result would be a higher than normal sympathetic efferent neural tone with, for instance, increased left ventricular output and possibly an enhanced total periperal vascular tone. The resultant complex resetting of multiple arterial baroreflexes presumably would be associated with resistance vessel remodeling [20] and altered arterial pressure [21] known to accompany essential hypertension.

ACKNOWLEDGMENTS

This work was supported by a grant from the Natural Sciences and Engineering Research Council of Canada, Canadian Institutes of Health Research, and the Heart and Stroke Foundation of Canada.

[1] K. M. Spyer, "Neural organization and control of the baroreceptor reflex" (unpublished); Rev. Physiol. Biochem. Pharmacol. **88**, 24 (1981).
[2] M. C. Andresen and D. L. Kunze, Annu. Rev. Physiol. **56**, 93 (1994).
[3] M. C. Andresen and M. Yang, Clin. Exp. Pharmacol. Physiol. **15**, 19 (1989).
[4] M. C. Andresen, J. M. Krauhs, and A. M. Brown, Circ. Res. **43**, 728 (1978).
[5] M. C. Andresen, S. Kuraoka, and A. M. Brown, Circ. Res. **47**, 821 (1980).
[6] M. W. Chapleau, Z. Li, S. S. Meyrelles, X. Ma, and F. M. Abboud, Ann. N.Y. Acad. Sci. **940**, 1 (2001).
[7] P. A. Lanfranchi and V. K. Somers, Am. J. Physiol. **283**, 815 (2002).
[8] J. A. Armour, Can. J. Physiol. Pharmacol. **63**, 704 (1985).
[9] J. A. Armour, Can. J. Physiol. Pharmacol. **64**, 101 (1986).
[10] M. H. Huang, R. M. Negoescu, M. Horackova, S. Wolf, and J. A. Armour, Cardiovasc. Res. **32**, 503 (1996).
[11] J. A. Armour, Am. J. Physiol. **225**, 177 (1973).
[12] A. C. Burton, Physiol. Rev. **34**, 619 (1954).
[13] J. A. Armour and G. C. Kember, *Basic and Clinical Neurocardiology* (Oxford University Press, New York, 2004).
[14] B. Duan and M. Zamir, J. Acoust. Soc. Am. **92**, 3358 (1992).
[15] B. Duan and M. Zamir, Ann. Biomed. Eng. **23**, 794 (1995).
[16] M. Zamir, *The Physics of Pulsatile Flow* (Springer-Verlag, New York, 2000).
[17] M. Zamir, Comments Theoretical Biology **1**, 15 (1998).
[18] W. W. Nichols and W. F. O'Rourke, *McDonald's Blood Flow in Arteries* (Arnold, London, 1998).
[19] J. A. Armour and J. L. Ardell, *Neurocardiology*, (Oxford University Press, New York, 1994).
[20] M. J. Mulvany, News Physiol. Sci. **17**, 105 (2002).
[21] G. F. DiBona, Hypertension **43**, 147 (2004).